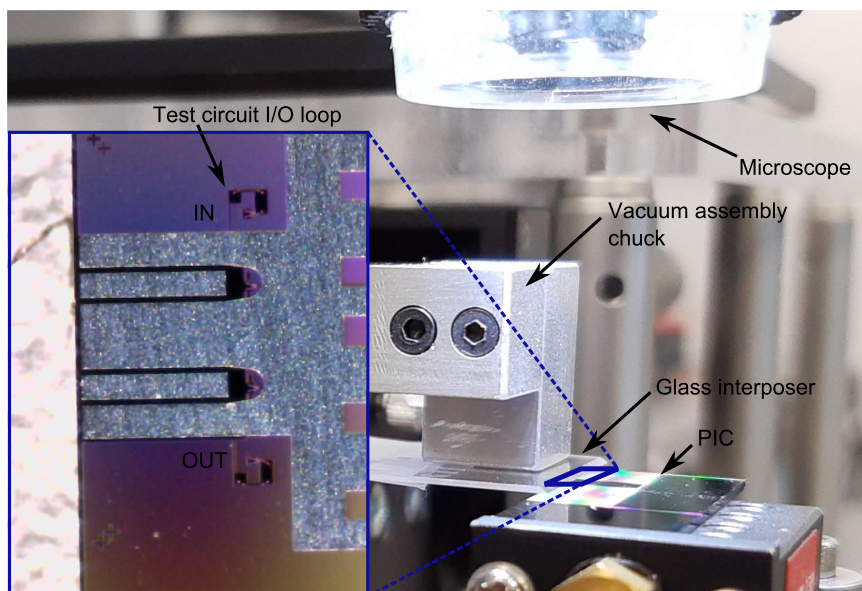


Laser Written Glass Interposer for Fiber Coupling to Silicon Photonic Integrated Circuits

Volume 13, Number 1, February 2021

A. Desmet
A. Radosavljević
J. Missinne
D. Van Thourhout
G. Van Steenberge



DOI: 10.1109/JPHOT.2020.3039900

Laser Written Glass Interposer for Fiber Coupling to Silicon Photonic Integrated Circuits

A. Desmet ^{1,2}, A. Radosavljević ^{1,2}, J. Missinne ¹,
D. Van Thourhout ² and G. Van Steenberge ¹

¹Centre for Microsystems Technology (CMST), Department of Electronics and Information Systems (ELIS), Ghent University - imec, 9052 Gent, Belgium

²Photonics Research Group (PRG), Department of Information Technology (INTEC), Ghent University - imec, 9052 Gent, Belgium

DOI:10.1109/JPHOT.2020.3039900

This work is licensed under a Creative Commons Attribution 4.0 License. For more information, see <https://creativecommons.org/licenses/by/4.0/>

Manuscript received October 5, 2020; revised November 12, 2020; accepted November 18, 2020. Date of publication November 24, 2020; date of current version December 31, 2020. This work was supported in part by the Special Research Fund of Ghent University under Grant BOF14/GOA/034 project and in part by the Hercules Foundation Flanders under Grant ZW09-01: APPLIE4MOS. Corresponding author: G. Van Steenberge (e-mail: Geert.VanSteenberge@UGent.be).

Abstract: Recent advancements in photonic-electronic integration push towards denser multichannel fiber to silicon photonic chip coupling solutions. However, current packaging schemes based on suitably polished fiber arrays do not provide sufficient scalability. Alternatively, lithographically-patterned fused silica glass interposers have been proposed, allowing for the integration of fanout waveguides between a dense array of on-chip silicon waveguides and a cleaved fiber ribbon. In this paper, we propose the use of femtosecond laser inscription for the fabrication of the fused silica glass interposer, allowing for a monolithic integration of waveguides and V-grooves for fiber alignment. The waveguides obtained by Femtosecond Laser Direct Writing (FLDW) have a propagation loss of 0.88 dB/cm at 1550 nm. The mode-field diameter is $12.8 \pm 0.4 \mu\text{m}$, allowing for a coupling loss of 1.24 ± 0.32 dB when coupling to a standard single mode optical fiber, passively aligned to the fused silica waveguide by insertion in a V-groove created by Femtosecond Laser Irradiation followed by Chemical Etching (FLICE). The average surface roughness of the etched waveguide facet is 160 ± 5 nm. Scattering loss when coupling to fiber is reduced by use of an index-matching adhesive for fiber fixation. A polished out-of-plane coupling mirror at an angle of 41.5° injects the light into standard grating couplers, providing a quasi-planar fiber-to-chip package. The excess loss of the proposed solution is limited to 2 dB per interface, including mirror, waveguide and fiber coupling losses.

Index Terms: Glass interposer, integrated photonics, photonics packaging, ultrafast laser inscription.

1. Introduction

Fiber-To-Chip coupling is a key aspect of silicon photonics chip packaging, with multiple figures of merit such as coupling efficiency, bandwidth, polarization dependence, input/output (I/O) density and alignment tolerance. Current solutions can be broadly divided into two principle categories: out-of-plane coupling using grating couplers (GC) and in-plane or edge coupling [1]. Single polarization GCs with insertion loss below 1 dB for coupling to standard optical fibers have been reported [2], but typical insertion loss of multi-project-wafer fabricated grating couplers is 2.5 dB

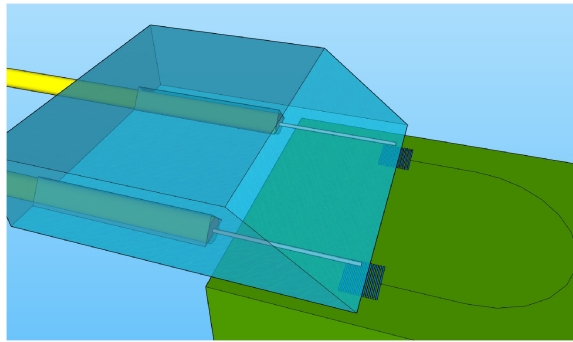


Fig. 1. Schematic of the test vehicle, representing fiber to silicon photonic chip coupling through a fused silica glass interposer fabricated using femtosecond laser inscription.

(C-band, TE polarization), featuring a 1 dB bandwidth of 29 nm [3]. Recently, grating couplers with downward directionality were reported [4], enabling new schemes for optical coupling [5] and 3D electro-optic integration [6]. Edge coupling provides a relatively high coupling efficiency of -2 dB to lensed fibers, a 1 dB bandwidth of more than 100 nm, and a low polarization dependent loss (<0.5 dB) [3]. However, the larger mode field diameter of a grating coupler as compared to a typical edge coupling scenario results in an increased alignment tolerance during assembly, which becomes increasingly important for multichannel fiber-to-chip coupling. As a result, grating couplers are still the mainstream approach for coupling to fiber arrays, for which the standardized approach is to precisely align several fibers in V-grooves etched into a glass or silicon block, polished to a common optical facet [1]. In order to reduce the fiber array footprint on the photonic chip and improve the form factor of the packaged device, total internal reflection from a suitably polished fiber surface is used to direct the beam into a GC at the required angle. While this solution offers low loss, with a 1 dB roll tolerance of 2.5° in addition to a 1 dB lateral alignment tolerance of $\pm 2.5 \mu\text{m}$ [7], it requires angle-polishing of fibers which is impractical and limits throughput. Moreover, the achievable channel pitch is limited to 127 or $250 \mu\text{m}$, dictated by the optical fiber outer cladding diameter. To circumvent these limitations, lithographically patterned fused silica interposers have been proposed, integrating fanout waveguides between a dense array of on-chip silicon waveguides and a fiber array [8].

We propose a silicon photonic chip packaging solution based on a fused silica glass interposer, in which both optical and mechanical structures are defined using femtosecond laser inscription. When fused silica is irradiated by tightly focused femtosecond laser pulses, permanent modification occurs. This is due to multiphoton absorption in otherwise transparent glass, which is achieved by the very high peak intensities of the strongly focused ultrashort laser pulses. After the energy of the laser pulse is absorbed, the material relaxes, resulting in permanent modification of the glass. Davis *et al.* showed in 1996 that it is possible to create optical waveguides in arbitrary 3D paths in glass based on this technique [9]. This fast and straightforward Femtosecond Laser Direct Writing (FLDW) technology allows for fused silica waveguides with low propagation losses and mode field diameters comparable with single mode fibers [10], which makes them suitable for photonics packaging. On the other hand, by locally illuminating the glass using femtosecond laser pulses, the selectivity to etching agents can drastically be increased which allows removing desired volumes of glass, a process known as Femtosecond Laser Irradiation followed by Chemical Etching (FLICE) [11]. Using FLICE, it is possible to create opto-mechanical structures with arbitrary shapes [12].

Combining FLDW with FLICE allows for the simultaneous inscription of waveguides and V-grooves in fused silica, with mutually high alignment accuracy. A schematic representation of the photonics packaging test vehicle used throughout the paper is shown in Fig. 1. The silicon photonic test chip having a waveguide loop between 2 grating couplers, the fused silica optical interposer

and the optical fiber interface are illustrated. While in principle the FLICE technique can also be used for the creation of the out-of-plane coupling mirror, we have used mechanical polishing during this work, resulting in a reduced mirror surface roughness.

The focus of the paper is on the optical coupling part, but the proposed concept offers important advantages with respect to scalability. The straight waveguides implemented on the current test vehicle can easily be replaced by a fanout from a more dense array of silicon waveguides towards a more coarse array of optical fibers, either in a linear or multicore fiber configuration [13]. In addition, the fabrication of the optical interposer can be completed on wafer-level, assuming the use of FLICE for the definition of the out-of-plane coupling mirror, possibly combined with an additional surface treatment step. While active alignment is used during assembly of the test vehicle, the assembly of the interposer on the photonic chip is compatible with passive assembly, owing to the possibility to integrate visual alignment markers using the FLICE technology.

2. Methods

2.1 General

We use a commercial ytterbium-doped fiber laser (Satsuma, Amplitude Systèmes) to fabricate single mode optical waveguides and V-grooves, integrated together on a single glass substrate. The lasing frequency is doubled from 1030 nm to 515 nm using a second harmonic generation (SHG) module to achieve more efficient laser processing of wide-bandgap fused silica by reducing the order of the multiphoton absorption [14]. Pulse length is <400 fs and the repetition rate is set to 500 kHz. The linearly polarized laser beam is focused onto a high purity 500 μm thick fused silica substrate from Siegert with a 0.55 NA aspheric lens (Newport 5722-A-H). The power of the femtosecond laser is controlled with an automated rotatable half-wave plate and a linear polarizer. Average laser powers ranging from 25 mW to 350 mW are measured after focusing. The samples are placed on a computer-controlled motorized XY stage that is translated perpendicularly to the laser beam. Changes in writing depth are achieved by moving the objective closer to the sample.

During the femtosecond laser inscription step, the V-grooves and waveguides are defined simultaneously, providing a proper mutual alignment. To allow for low-loss optical coupling between the optical fiber and the laser written waveguide, the end-face of the V-groove is written along the direction perpendicular to the femtosecond laser polarisation, which allows for the lowest facet roughness. As the laser polarisation is kept fixed during the process, the waveguides are written along the direction parallel to the laser polarisation, which leads to the lowest waveguide propagation loss [15]. In a second step, the fused silica substrate is submerged into an aqueous KOH solution so that the V-grooves are etched. The angled waveguide end-face is obtained by mechanical polishing. The fabrication of the glass interposer is now completed, and after singulation by dicing, the optical fibers are assembled in the V-groove, allowing for intermediate coupling loss measurements. Finally, the interposer is assembled onto the silicon photonic test chip.

2.2 Femtosecond Laser Waveguide Writing

Single mode optical waveguides are written with a stage translation speed of 0.5 mm/s, and a laser power of 125 mW, resulting in a mode field diameter matching to single mode fiber and an acceptable waveguide propagation loss [15]. The waveguides are defined 43 μm below the surface, matched to the V-groove design as described in the next section.

2.3 V-Groove Fabrication

The laser written V-grooves are designed for compatibility with standard single mode fiber (SMF-28) having a cladding diameter of 125 μm . To avoid stress concentrations around sharp tips, the V-groove is designed to have a flat bottom surface. The depth is optimized such that the matching waveguides properly guide light, but at the same time the V-groove should allow for passive

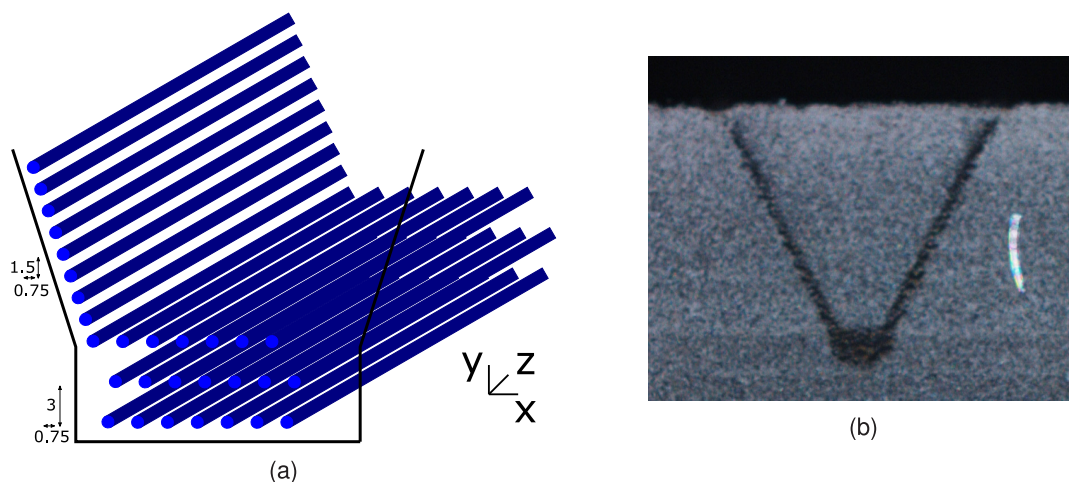


Fig. 2. (a) Stacking of individual laser lines along the contours of the designed V-groove. Pitch between individual lines is $0.75 \mu\text{m}$ in X- and $1.5 \mu\text{m}$ in Y-direction. The bottom of the groove has been exposed 3 times with a pitch of $3 \mu\text{m}$ in Y-direction. Note that not all laser lines are drawn. (b) Optical microscope image after laser exposure showing the contours of the V-groove cross-section.

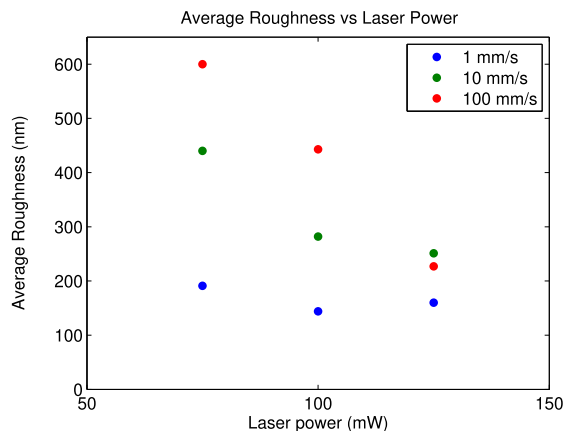


Fig. 3. Surface roughness as function of femtosecond laser power and laser scanning speed.

assembly of SMF-28 fiber, sufficiently protruding the surface of the optical interposer, so that it can easily be aligned in the vertical direction from the top. Angled sidewalls are formed by scanning single laser tracks from bottom to top, with a horizontal and vertical separation of $0.75 \mu\text{m}$ and $1.5 \mu\text{m}$ respectively, leading to a 63.2° angle, as represented in Fig. 2(a). The flat bottom section of the V-groove contains 3 planes of lines stacked on top of each other, with a pitch of $3 \mu\text{m}$. This allows to lift-off the inner part of the V-groove, during the wet chemical etching. By only irradiating the contours of the V-groove, instead of the entire 3D volume, the overall exposure time is significantly reduced. To fully enclose the volume, the end-face of the V-groove is created by scanning multiple lines from top to bottom in the X-direction with a pitch of $1 \mu\text{m}$ in the Y-direction.

For the irradiation of the V-groove contours, a laser power of 100 mW and a writing speed of 100 mm/s is used, allowing for a controlled etching of the entire V-groove with a good trade-off between processing speed and resulting surface roughness. A picture of the cross-section of a V-groove after the laser inscription process is shown in Fig. 2(b). For the definition of the V-groove end-face, interfacing with the optical waveguide, lines are scanned at a reduced speed of 1 mm/s with a smaller pitch in the Y-direction, resulting in a better waveguide end-face surface roughness. See Fig. 3, in which the surface roughness is plotted as a function of laser writing speed and laser

power (measured using a white-light Vertical Scanning Interferometric (VSI) optical profiler, Wyko NT3300). Using the selected laser writing parameters, the time required for exposing a 10 mm long V-groove is less than 1 minute. After completing the laser exposure step, the fused silica sample is submerged into a 30% KOH solution for 4 hours at 85 °C after which the KOH container with the sample is put into an ultrasonic bath for 30 minutes. The ultrasonic bath gives a more reliable etching for structures of which only the contours have been exposed. Most likely, the ultrasonic agitation provides a better penetration and refreshment of the etchant in the narrow channels which are being etched. To avoid waveguide etching, the distance between the start of the optical waveguide and the V-groove end-face was set at 10 μm .

2.4 Mirror Fabrication

In order to deflect the beam from a surface-parallel direction (optical fibers) to a 7° angle (in silica) for compatibility with standard silicon photonics grating couplers, an angle of 41.5° is required for the out-of-plane coupling mirror. The mirror is created by placing the fused silica substrate into a holder with a predetermined angle of 41.5°. The glass sample is ground and polished with decreasing roughness of abrasive silicon carbide grinding paper (P1200 and P4000). For the last polishing step a sludge with 50 nm colloidal silica is used.

2.5 Assembly of the Glass Interposer

The assembly of the device shown in Fig. 1 contains two steps: (1) Inserting optical fibers in the V-grooves and fixing it with a UV-curable glue (NOA65). (2) Flipping the glass substrate and actively aligning it to the silicon photonics grating couplers. The substrate is flipped so that the distance the light needs to travel from the mirror to the GC is minimized, reducing loss due to diffraction. Once active alignment is completed, the glass substrate can be fixed using UV-curable glue.

2.6 Characterization Setup

Firstly, the laser-written waveguides themselves were characterized. Therefore, a 1.5 cm long waveguide was prepared of which both end-faces were polished, which allows butt coupling with single mode fibers. The total insertion loss was obtained by launching light ($\lambda = 1550$ nm) from a pigtailed laser diode using a single mode fiber actively aligned at the waveguide input and collecting the transmitted power at the output using another single mode fiber connected to a power meter. The waveguide mode field diameter was obtained by imaging the end-face of the waveguide using an infrared camera (Xenics Xeva), while light was launched from the input. This allows recording the waveguide mode field diameter and as such estimating the minimum achievable coupling loss. The waveguide propagation loss on the other hand, was obtained using Optical Frequency Domain Reflectometry (LUNA OVA 5000) [16], according to the procedure detailed in [15]. To allow for a reliable waveguide loss measurement, a 10 cm long waveguide sample was prepared, using the laser settings as detailed in Section 2.2.

Secondly, the coupling loss between the laser-written waveguide and an SMF-28 fiber, aligned in a V-groove, was measured. Therefore, V-grooves were realized in line with laser-written waveguides, with a varying offset in height with respect to the ideal coupling position. The other end-face of the sample was polished. The total insertion loss was obtained by launching 1550 nm light in an SMF-28 fiber mounted in the different V-grooves and collecting the transmitted light from the polished end-face with another SMF-28 fiber. By taking into account the waveguide propagation loss and coupling loss at the output end-face, the coupling loss between waveguide and fiber mounted in V-groove can be extracted.

Thirdly, the additional loss induced by the polished mirror is obtained using an input fiber mounted in a V-groove and output fiber under the correct angle above the mirror.

Finally, the glass interposer with polished mirror and 2 mounted fibers was aligned above the test site of the PIC and the total insertion loss was recorded. The used PIC was fabricated via

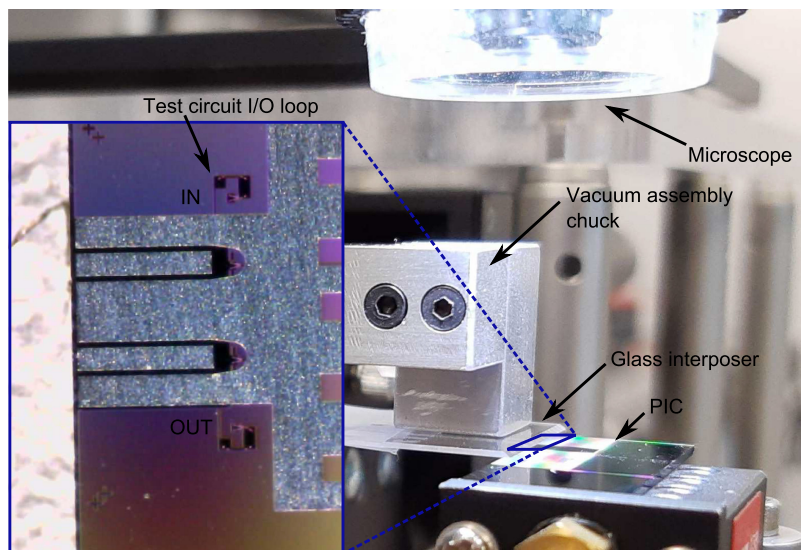


Fig. 4. Setup used to align and mount the glass interposer onto the PIC.

the Europractice MPW fabrication service and contained regular TE grating couplers for C-band operation (FGCCTE_FC1DC_625_313, 1558 nm peak wavelength at 10° coupling angle in air, approximately -4 dB peak insertion loss). To this end, the PIC was fixed on a first vacuum chuck and the glass interposer was fixed on a second vacuum chuck on an arm mounted on a 6-axis motorized alignment stage (Thorlabs Nanomax 606) which allowed aligning the interposer with respect to the input and output grating couplers, see Fig. 4. The first fiber was connected to a broadband source (Thorlabs ASE-FL7002) and the second fiber to an optical spectrum analyzer (Agilent 86142B). After active alignment, the insertion loss spectrum was obtained. In addition, a reference measurement was done, without glass interposer, but using 2 single mode fibers, aligned above 2 grating couplers under the 10° coupling angle in air (same grating couplers, on a different test site of the PIC).

3. Results and Discussion

3.1 Waveguide Loss

A microscope image of the cross-section of a fused silica waveguide defined by FLDW is presented in Fig. 5(a). The waveguide was written with the laser beam incident from the bottom, approximately $43 \mu\text{m}$ below the surface. The waveguiding region is located above the slightly darker region.

The waveguide mode field diameter was measured to be $12.8 \pm 0.4 \mu\text{m}$ in the lateral direction and $12.1 \pm 1.3 \mu\text{m}$ in the vertical direction using the $1/e^2$ intensity distribution method, see Fig. 5(b). The waveguides showed a polarization insensitive propagation loss of 0.88 dB/cm, measured by OFDR, see Fig. 6. On the other hand, the measured total insertion loss for a 1.5 cm waveguide was 2.17 ± 0.01 dB. Taking the obtained propagation loss into account, this results in an estimated fiber-to-waveguide coupling loss of 0.43 dB when actively aligned.

3.2 Coupling Performance of the V-Grooves for Passive Fiber Alignment

A cross-section of an etched V-groove is shown in Fig. 7. The width and slopes of the V-groove define the position of the optical fiber, protruding $19 \mu\text{m}$ from the top, to allow for a vertical alignment by pushing down using a lid. The fiber core is situated $43.5 \mu\text{m}$ under the surface of the glass, matching the height of the FLDW waveguides. The surface roughness of the V-groove end-face

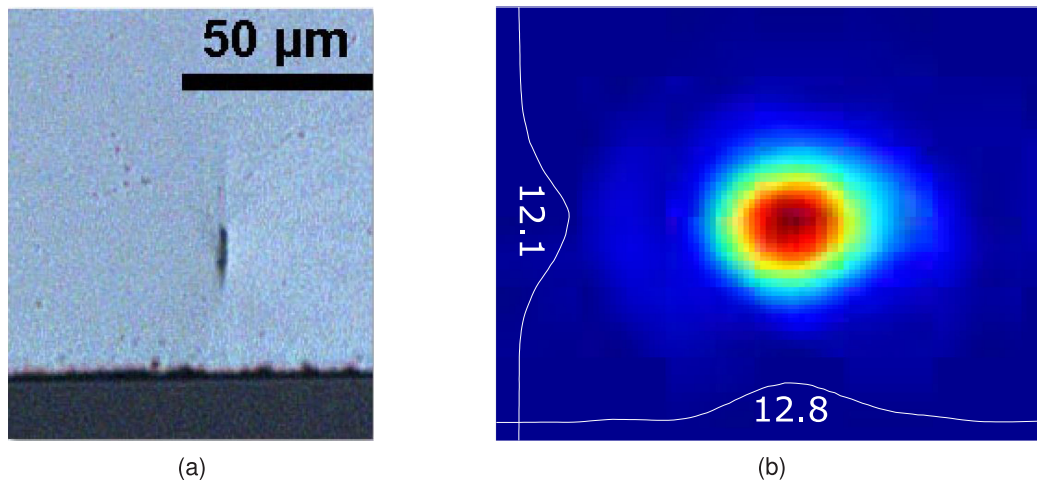


Fig. 5. (a) Optical microscope image of a fused silica substrate cross-section. The FLDW waveguide is located approximately $43 \mu\text{m}$ below the surface. (b) Waveguide mode intensity profile yielding a MFD ($1/e^2$ spot size) of $12.8 \mu\text{m}$ by $12.1 \mu\text{m}$ at 1550 nm .

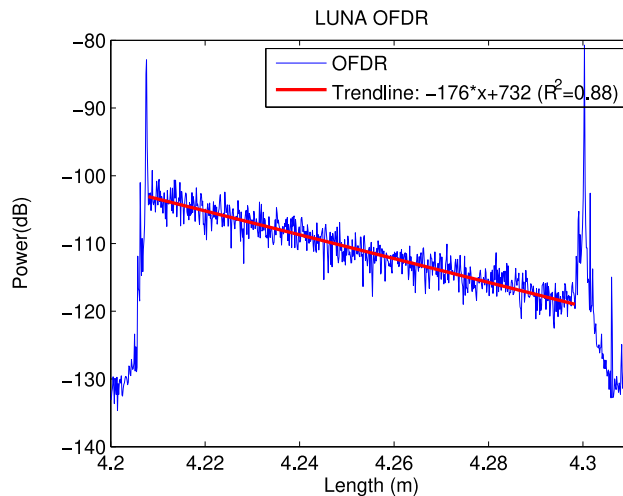


Fig. 6. OFDR measurement of waveguide propagation loss. The trendline shows a loss of 176 dB/m for after transmitting and reflecting light, which results in a (one-way) waveguide propagation loss of 0.88 dB/cm .

was measured using white light interferometry, yielding an average roughness R_a of $160 \pm 5 \text{ nm}$ (measured over a $45 \mu\text{m} \times 59 \mu\text{m}$ area).

The coupling loss from an optical fiber self-aligned and assembled in a V-groove to a 7.5 mm long femtosecond laser direct-written waveguide is presented in Fig. 8, for different waveguides showing an offset in height with respect to the V-groove. It can be seen that the coupling loss goes through a minimum ($1.24 \pm 0.32 \text{ dB}$, average value over 3 measurements) when the waveguide and V-groove are at the ideal offset with respect to each other and that the coupling loss increases when there is a mismatch in off-set (in both directions). The expected loss due to mode mismatch and lateral off-set are simulated using Lumerical Mode Solutions Finite Difference Eigenmode Solver. In case of perfect alignment, the loss equals 0.22 dB , caused by the mode mismatch. The difference between the simulated coupling loss at the optimum position (0.22 dB), and the measured loss (1.24 dB), could be explained by a slight lateral off-set of the fiber with respect to the waveguide

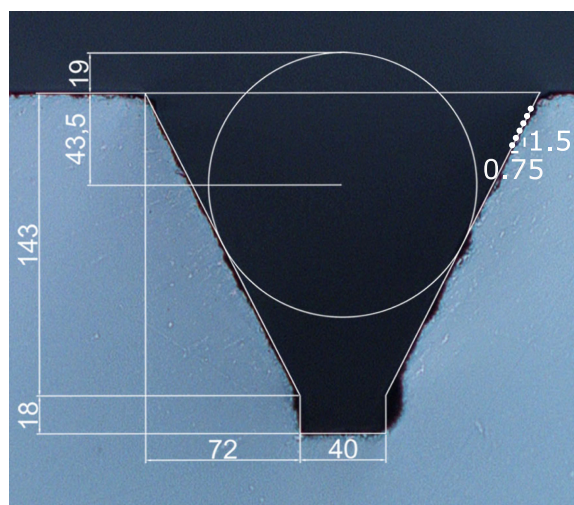


Fig. 7. Optical microscope image after making a V-groove cross-section. Dimensions in micro meter. The circle represents the location of an optical fiber assembled in the V-groove, matching the waveguide depth, $43.5 \mu\text{m}$ below the surface. Angled sidewalls are formed by scanning single laser tracks from bottom to top, with a horizontal and vertical separation of $0.75 \mu\text{m}$ and $1.5 \mu\text{m}$ respectively, leading to a 63.2° angle.

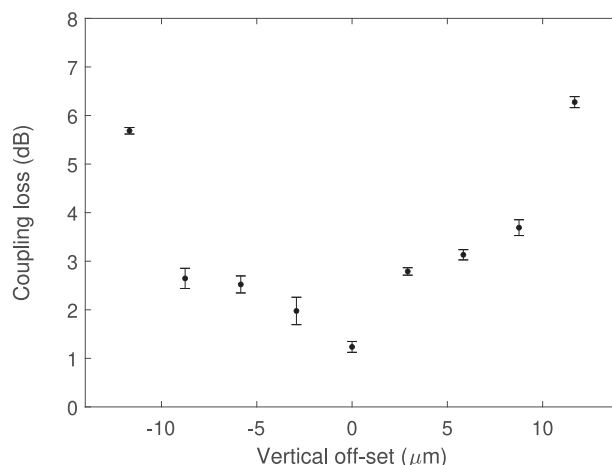


Fig. 8. Coupling loss between self-aligned fibers assembled in V-grooves and fused silica waveguides for an increasing off-set in height. Relative error bars are included.

(simulated loss of 1 dB per $2.5 \mu\text{m}$ lateral shift), scattering loss due to surface roughness, and the longitudinal off-set between fiber and waveguide facet.

The process to create V-grooves and waveguides can easily be scaled to higher channel counts, required in e.g. an optical transceiver. To illustrate this, five identical V-grooves and waveguides with a pitch of $250 \mu\text{m}$ were defined, allowing for passive assembly of an array of fibers. A microscope image showing this V-groove array from the top can be seen in Fig. 9. The pitch, number of V-grooves in the array, and optical waveguide layout can easily be adapted, and scaled to match any optical fiber ribbon. Table 1 shows the results of the total transmission loss measurements after assembly of the optical fibers, leading to an average insertion loss of $2.15 \pm 0.15 \text{ dB}$, including the coupling loss from the input fiber (mounted in the V-groove) to optical waveguide, waveguide propagation loss, and coupling loss to the actively aligned output fiber.

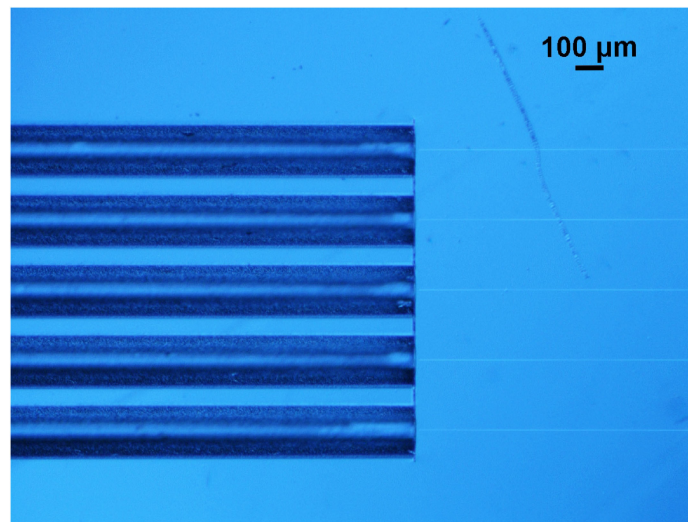


Fig. 9. Differential Interference Contrast microscopic image of an array of V-grooves and matching waveguides, after assembly of the fiber array.

TABLE 1

Total Insertion Loss (Fiber, Over Waveguide, to Fiber) for 5 V-Grooves in an Array As Shown in Fig. 9. in Each Channel, the In-Coupling Fiber Was Passively Aligned in the V-Groove, and the Out-Coupling Fiber Was Actively Aligned to the Optical Waveguide Facet

	Insertion Loss (dB)
channel 1	2.28
channel 2	2.09
channel 3	2.09
channel 4	2.09
channel 5	2.03

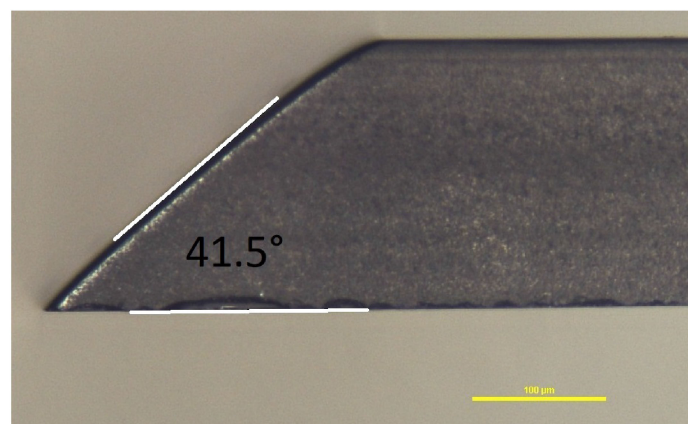


Fig. 10. Episcopic microscope image of the mirror cross-section, confirming the angle of 41.5° .

3.3 Mirror

A microscope image of the mirror cross-section is presented in Fig. 10 and confirms the angle of 41.5° , as designed to allow for compatibility with standard silicon photonics grating couplers (optimum coupling angle of 7° in oxide, or index matching adhesive). The average roughness of

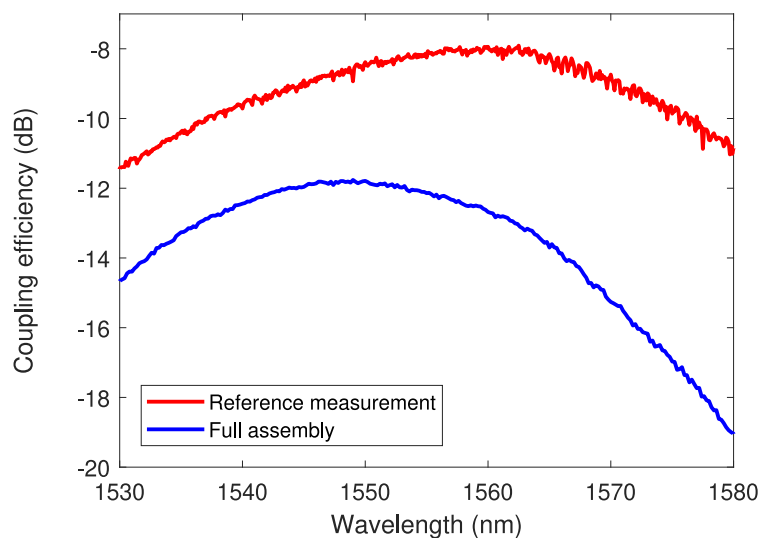


Fig. 11. Coupling efficiency measurements of the chip, in red, which represents the coupling efficiency of the grating couplers, and the full assembly, in blue, which shows the coupling efficiency for the chip combined with the glass interposer.

the polished mirror facet is 9 nm, measured over a $120 \mu\text{m} \times 92 \mu\text{m}$ area, using a red light Phase Shift Interferometric (PSI) optical profiler (Wyko NT3300).

After completing the mirror fabrication, the measured total insertion loss was 2.7 dB and 2.4 dB for 2 channels respectively. After curing the adhesive to fix the fibers in the V-grooves, the loss slightly increased to 2.8 dB and 2.5 dB respectively, which could be explained by an increased misalignment due to adhesive shrinkage during curing. Compared to the insertion loss values measured prior to the mirror polishing (2.15 ± 0.15 dB), the additional loss introduced by the out-of-plane coupling mirror is between 0.25 and 0.55 dB. Compared to lithographically patterned fused silica interposer solutions (e.g. [8]), we end up with a higher insertion loss (2.5–2.8 dB versus 0.6–1.2 dB), but our solution allows for passive alignment of optical fibers in the monolithically integrated V-grooves.

3.4 Characterization of the Full Assembly

Fig. 11 shows the total insertion loss of the reference measurement (chip) together with the total insertion loss of the full assembly (chip + interposer). By means of comparison, both measurements were done without adhesive fixation. First, it can be observed that the reference spectrum (10° coupling angle in air) shows the peak coupling efficiency at approximately 1560 nm (-7.9 dB) together with a 1 dB bandwidth of 26 nm which is very close to the grating coupler specifications. In case of the intermediate glass interposer, the peak coupling efficiency is at 1550 nm (-11.8 dB), with a 1 dB bandwidth of 22 nm. The difference in peak wavelength is due to the slightly different coupling angle, either caused by a slight deviation of the mirror angle or a tilt of the glass interposer when assembled above the grating couplers. The reduction in bandwidth on the other hand, could be caused by the slightly lower numerical aperture of the glass waveguides (NA of 0.11, compared to 0.14 for SMF-28). Second, assuming the short Si waveguide sections have similar, negligible loss in both cases, the additional loss caused by the glass interposer can be obtained by comparing both insertion loss curves, taking into account the spectral shift. As a result, an additional loss of 3.9 dB is calculated for two fiber-to-PIC interfaces, corresponding to an additional loss of ~ 2 dB per interface. Although the obtained loss is in line with the insertion loss measurements of the glass interposer reported in Section 3.3, there is a deviation of 0.5–0.8 dB. This might be explained simply by measurement inaccuracies, or possibly by a higher coupling efficiency between grating

TABLE 2

Loss Contributions of the Various Interfaces of the Laser Written Fused Silica Interposer

	Loss
waveguide propagation	0.88 dB/cm
fiber-to-waveguide coupling using active alignment	0.43 dB
fiber-to-waveguide coupling using V-groove assisted passive alignment	1.24 dB
out-of-plane coupling mirror	0.25-0.55 dB
interposer after assembly on silicon PIC	2 dB per interface

coupler and glass waveguide (compared to fiber), given the slightly larger and asymmetric mode of the FLDW waveguide. The main loss contributions of the various interfaces have been summarized in Table 2.

4. Conclusion

We described a scalable method for coupling to silicon photonic integrated circuits, using a silica-based optical interposer containing optical waveguides and mechanical alignment structures, monolithically integrated, owing to the capabilities of the fabrication technique based on ultrafast laser inscription. The waveguides defined using Femtosecond Laser Direct Writing (FLDW) have a propagation loss of 0.88 dB/cm, and a coupling loss to SMF-28 of 0.43 dB. After passive assembly of an optical fiber in a V-groove defined using Femtosecond Laser Irradiation followed by Chemical Etching (FLICE), the obtained coupling loss was 1.24 dB. After polishing an out-of-plane coupling mirror at an angle of 41.5° , the insertion loss increased to 2.5–2.8 dB. The interposer was assembled on a silicon photonic test chip, containing a waveguide loop. The total insertion loss of the full assembly was 11.8 dB at 1550 nm, corresponding to an increased loss of 2 dB per interface compared to direct fiber-to-PIC coupling, which could be further reduced by fine-tuning the FLDW and FLICE process. Using the currently optimized laser parameters, the time required to expose a single V-groove/waveguide combination is around one minute. Although the content of the paper focuses on the fabrication and characterization of the interposer, more complex fanout waveguide designs could be integrated, proving the full-potential of the proposed technique with respect to scalability.

References

- [1] R. Marchetti, C. Lacava, L. Carroll, K. Gradkowski, and P. Minzioni, "Coupling strategies for silicon photonics integrated chips (invited)," *Photon. Res.*, vol. 7, no. 2, pp. 201–239, Feb. 2019.
- [2] W. S. Zaoui *et al.*, "Bridging the gap between optical fibers and silicon photonic integrated circuits," *Opt. Exp.*, vol. 22, no. 2, pp. 1277–1286, Jan. 2014.
- [3] Imec, "Photonic integrated circuit prototyping and small volume production," Accessed: Dec. 2020. [Online]. Available: <https://www.imec-int.com/en/what-we-offer/ic-link/photonic-integrated-circuits>
- [4] N. Mangal, J. Missinne, G. V. Steenberge, J. V. Campenhout, and B. Snyder, "Performance evaluation of backside emitting o-band grating couplers for 100- μ m-thick silicon photonics interposers," *IEEE Photon. J.*, vol. 11, no. 3, Jun. 2019.
- [5] N. Mangal, B. Snyder, J. V. Campenhout, G. V. Steenberge, and J. Missinne, "Expanded-beam backside coupling interface for alignment-tolerant packaging of silicon photonics," *IEEE J. Sel. Topics Quantum Electron.*, vol. 26, no. 2, pp. 1–7, Mar./Apr. 2020.
- [6] N. Mangal, J. Missinne, J. V. Campenhout, B. Snyder, and G. V. Steenberge, "Ball lens embedded through-package via to enable backside coupling between silicon photonics interposer and board-level interconnects," *J. Lightw. Technol.*, vol. 38, no. 8, pp. 2360–2369, Apr. 2020.
- [7] B. Snyder and P. O'Brien, "Packaging process for grating-coupled silicon photonic waveguides using angle-polished fibers," *IEEE Trans. Compon., Packag. Manuf. Technol.*, vol. 3, no. 6, pp. 954–959, Jun. 2013.
- [8] H. Hwang *et al.*, "128 \times 128 silicon photonic mems switch package using glass interposer and pitch reducing fibre array," in *Proc. IEEE 19th Electron. Packag. Technol. Conf.*, 2017, pp. 1–4.
- [9] K. Davis, K. Miura, and K. Hirao, "Writing waveguides in glass with a femtosecond laser," *Opt. Lett.*, vol. 21, pp. 1729–1731, 1996.
- [10] L. Tong, R. R. Gattass, I. Maxwell, J. B. Ashcom, and E. Mazur, "Optical loss measurements in femtosecond laser written waveguides in glass," *Opt. Commun.*, vol. 259, no. 2, pp. 626–630, 2006.

- [11] R. R. Gattass and E. Mazur, "Femtosecond laser micromachining in transparent materials," *Nat. Photon.*, vol. 2, pp. 219–225, Apr. 2008.
- [12] A. Marcinkevičius *et al.*, "Femtosecond laser-assisted three-dimensional microfabrication in silica," *Opt. Lett.*, vol. 26, no. 5, pp. 277–279, Mar. 2001.
- [13] R. R. Thomson, R. J. Harris, T. A. Birks, G. Brown, J. Allington-Smith, and J. Bland-Hawthorn, "Ultrafast laser inscription of a 121-waveguide fan-out for astrophotonics," *Opt. Lett.*, vol. 37, no. 12, pp. 2331–2333, Jun. 2012.
- [14] L. Shah, A. Arai, S. Eaton, and P. Herman, "Waveguide writing in fused silica with a femtosecond fiber laser at 522 nm and 1 mhz repetition rate," *Opt. Exp.*, vol. 13, no. 6, pp. 1999–2006, Mar. 2005.
- [15] A. Radosavljević *et al.*, "Femtosecond laser-inscribed non-volatile integrated optical switch in fused silica based on microfluidics-controlled total internal reflection," *J. Lightw. Technol.*, vol. 38, no. 15, pp. 3965–3973, Aug. 2020.
- [16] B. J. Soller, D. K. Gifford, M. S. Wolfe, and M. E. Froggatt, "High resolution optical frequency domain reflectometry for characterization of components and assemblies," *Opt. Exp.*, vol. 13, no. 2, pp. 666–674, Jan. 2005.